

Network interactions within the canine intrinsic cardiac nervous system: implications for reflex control of regional cardiac function

Eric Beaumont¹, Siamak Salavatian², E. Marie Southerland¹, Alain Vinet^{2,3}, Vincent Jacquemet^{2,3}, J. Andrew Armour¹ and Jeffrey L. Ardell¹

¹Department of Biomedical Sciences, Quillen College of Medicine, East Tennessee State University, Johnson City, TN, USA

²Centre de Recherche, Hôpital du Sacré-Cœur, Montréal, QC, Canada

³Department of Physiology, Faculty of Medicine, Université de Montréal, Montréal, QC, Canada

Key points

- Control of regional cardiac function, as mediated by the intrinsic cardiac (IC) nervous system, is dependent upon its cardiac afferent neuronal inputs, changes in its central neuronal drive and interactions mediated within via local circuit neurons.
- The majority of its local circuit neurons receive indirect central (sympathetic and parasympathetic) inputs, lesser proportions transducing the cardiac milieu.
- Fifty per cent of IC neurons exhibit cardiac cycle-related periodicity that is primarily related to direct cardiac mechano-sensory afferent inputs and, secondarily, to indirect central autonomic efferent inputs.
- In response to mediastinal nerve stimulation, most IC neurons became excessively activated in the induction of atrial arrhythmias such that their stochastic interactivity precedes and persists throughout neuronally induced atrial fibrillation.
- Modulation of such stochastic IC local circuit neuronal recruitment may represent a novel target for the treatment of select cardiac disease, including atrial arrhythmias.

Abstract The aims of the study were to determine how aggregates of intrinsic cardiac (IC) neurons transduce the cardiovascular milieu *versus* responding to changes in central neuronal drive and to determine IC network interactions subsequent to induced neural imbalances in the genesis of atrial fibrillation (AF). Activity from multiple IC neurons in the right atrial ganglionated plexus was recorded in eight anaesthetized canines using a 16-channel linear microelectrode array. Induced changes in IC neuronal activity were evaluated in response to: (1) focal cardiac mechanical distortion; (2) electrical activation of cervical vagi or stellate ganglia; (3) occlusion of the inferior vena cava or thoracic aorta; (4) transient ventricular ischaemia, and (5) neurally induced AF. Low level activity (ranging from 0 to 2.7 Hz) generated by 92 neurons was identified in basal states, activities that displayed functional interconnectivity. The majority (56%) of IC neurons so identified received indirect central inputs (vagus alone: 25%; stellate ganglion alone: 27%; both: 48%). Fifty per cent transduced the cardiac milieu responding to multimodal stressors applied to the great vessels or heart. Fifty per cent of IC neurons exhibited cardiac cycle periodicity, with activity occurring primarily in late diastole into isovolumetric contraction. Cardiac-related activity in IC neurons was primarily related to direct cardiac mechano-sensory inputs and indirect autonomic efferent inputs. In response to mediastinal nerve stimulation, most IC neurons became excessively activated; such network behaviour preceded and persisted throughout AF. It was

concluded that stochastic interactions occur among IC local circuit neuronal populations in the control of regional cardiac function. Modulation of IC local circuit neuronal recruitment may represent a novel approach for the treatment of cardiac disease, including atrial arrhythmias.

(Received 27 May 2013; accepted after revision 24 June 2013; first published online 1 July 2013)

Corresponding author J. L. Ardell: Department of Biomedical Sciences, East Tennessee State University, Johnson City, TN 37614-0577, USA. Email: ardellj@etsu.edu

Abbreviations AF, atrial fibrillation; Ao, aortic; CAO, coronary artery occlusion; CV, cardiovascular; IC, intrinsic cardiac; ICNS, intrinsic cardiac nervous system; IVC, inferior vena cava; LAD, left anterior descending coronary artery; LCN, local circuit neuron; LCV, left cervical vagosympathetic complex; LMA, linear microarray; LSS, left stellate ganglion stimulation; LV, left ventricle; LVP, left ventricular pressure; MNS, mediastinal nerve stimulation; Occl, occlusion; RAGP, right atrial ganglionated plexus; RCV, right cervical vagosympathetic complex; RSS, right stellate ganglion stimulation; RV, right ventricle.

Introduction

It has been proposed that the intrinsic cardiac nervous system (ICNS) acts as the final coordinator of regional cardiac indices, doing so under the modulating influence of higher centres of the cardiac nervous system including intrathoracic-, spinal- and brainstem-mediated reflexes (Armour & Janes, 1988; Armour & Hopkins, 1990; Zucker & Gilmore, 1991; Ardell, 2004; Gray *et al.* 2004*b*). Coordination occurring within the ICNS is dependent on three factors: convergence of afferent neuronal inputs (mechano-sensitive, chemo-sensitive, ischaemic sensitive), central efferent neuronal inputs (both sympathetic and parasympathetic) and inter-connections mediated via local circuit neurons (Ardell *et al.* 1991; Armour *et al.* 1998; Taylor *et al.* 1999; Gray *et al.* 2004*a*; Herring & Paterson, 2009; McAllen *et al.* 2011). The latter neuronal population probably subserves complex reflex processing within the ICNS (Armour, 2008). Neuronal imbalances within any of these elements can exert deleterious effects on cardiac function, including arrhythmia induction (e.g. AF; (Scherlag *et al.* 2006; Shen *et al.* 2011; Gibbons *et al.* 2012)) and progression into congestive heart failure (Dell'Italia & Ardell, 2004; Liu *et al.* 2012; Zucker *et al.* 2012).

In order to characterize the ability of different neuronal populations within the ICNS to transduce altered cardiac status, the correlative interactions exhibited among specific IC neuronal populations within the heart need to be assessed with respect to whether they receive common shared cardiovascular sensory inputs or not (Thompson *et al.* 2000; Kember *et al.* 2001; Armour & Kember, 2004) as well as how they are impacted by central neuronal inputs (Ardell, 2004; Andresen *et al.* 2004; Herring & Paterson, 2009; McAllen *et al.* 2011). This information would form the basis for determining: (1) how they differentially transduce afferent inputs from different cardiac regions and the major thoracic vasculature (Thompson *et al.* 2000; Waldmann *et al.* 2006); (2) how individual neurons distributed throughout an intrinsic cardiac ganglionated plexus interact under the direct

versus indirect control of central cholinergic preganglionic (medullary) or adrenergic (spinal cord/stellate/middle cervical ganglia) efferent neuronal inputs (Gagliardi *et al.* 1988; Armour & Hopkins, 1990; Armour *et al.* 2002); and (3) how their sensory activity and interactive behaviour are affected by transient regional ventricular ischaemia (Huang *et al.* 1993; Armour *et al.* 1998, 2002). These questions have implications for atrial and ventricular arrhythmia induction which might arise as a consequence of abnormal interactions among the various populations of intrinsic cardiac neurons (Cardinal *et al.* 2009), an issue yet to be defined.

The present study addresses these questions in the anaesthetized canine preparation. With the emergence of linear microarray electrode technology, it is now feasible to evaluate *in situ* activities within and between different aggregates of IC neurons over relatively long periods of time, including in response to complex afferent and efferent stressors. Data so derived indicate that the majority of neurons in the ICNS are local circuit neurons that simultaneously transduce inputs from cardiac and major intrathoracic vascular receptors, as well as direct or indirect inputs from central (spinal cord and medullary) neurons. Surprisingly few IC neurons proved to be under the direct (monosynaptic) influence of medullary or spinal cord efferent preganglionic neurons. The interactive behaviour displayed among most of this ICNS network was of a primarily stochastic nature. Imbalance of intrinsic cardiac control in the induction of atrial arrhythmia indicates that targeting excessive, stochastic interactions among intrinsic cardiac local circuit neurons may be relevant to understanding how to mitigate such pathology therapeutically.

Methods

Ethical approval

Eight mongrel dogs (either sex), weighing 18–27 kg, were used in this study. All experiments were

performed in accordance with the guidelines for animal experimentation described in the 'Guiding principles for research involving animals and human beings' (World Medical Association; American Physiological Society, 2002). The Institutional Animal Care and Use Committee of East Tennessee State University approved these experiments.

Animal preparation

Animals were pre-medicated with sodium thiopental (15 mg kg^{-1} , i.v.), intubated and anaesthetized using 2% isoflurane. The left femoral vein was catheterized to allow fluid replacement as well as the administration of anaesthetic and pharmacological agents. Left ventricular chamber pressure was measured via a 5-Fr Mikro-Tip pressure transducer catheter (Millar Instruments, Houston, TX, USA) inserted into the chamber via the left femoral artery. The right femoral artery was catheterized to monitor aortic pressure using another Mikro-Tip transducer. Heart rate was monitored via ECG lead II. Depth of anaesthesia was assessed by monitoring corneal reflexes, jaw tone and alterations in cardiovascular indices. Following completion of the surgery, anaesthesia was changed to α -chloralose (75 mg kg^{-1} i.v. bolus), with continuous infusion ($16 \text{ mg kg}^{-1} \text{ h}^{-1}$) adjusted as required throughout the duration of each study. Body temperature was monitored rectally and maintained steady via a circulating water heating pad (T/Pump, Gaymar Industries Inc., Orchard Park, NY, USA). Respiration was controlled using an artificial ventilator (at $12\text{--}16 \text{ cycles min}^{-1}$) supplied with oxygen. Acid–base status was evaluated hourly (Irma TruePoint blood gas analyser, International Technidyne Corp., Edison, NJ, USA); tidal volume was adjusted and bicarbonate infused as necessary to maintain blood gas homeostasis.

Neuronal activity recording

Following a transthoracic thoracotomy (T4), a pericardial cradle was formed. The activity generated by neurons located in the right atrial ganglionated plexus (RAGP) was recorded *in situ* by means of a multichannel linear micro-electrode array (MicroProbes Inc., Guithersburg, MD, USA). This microelectrode linear array, consisting of 16 platinum/iridium electrodes ($25 \mu\text{m}$ diameter electrode with an exposed tip of 2 mm; impedance $0.3\text{--}0.5 \text{ M}\Omega$ at 1 kHz), was embedded in the right atrial fat that contained the RAGP such that its tip was placed adjacent to right atrial musculature.

The probe was attached to a flexible lead, allowing the probe to be semi-floating. The density of tissue in the ventral right atrial fat helped to maintain position stability over prolonged periods of time (6–8 h of recording).

The connecting wires of the multichannel electrode, along with earth and reference wires, were attached to a 16-channel microelectrode amplifier with headstage pre-amplifier (A-M systems, Inc., model 3600; Carlsborg, WA, USA). For each channel, filters were set to 300 Hz to 3 kHz, and gain to 5K. A hook electrode was sewn to the atrial myocardium close to the RAGP to provide a reference right atrial electrogram. This atrial electrogram was utilized for determination of atrial rate, duration and characterization of atrial arrhythmias, including atrial fibrillation, and for identification of the timing of atrial electrical artifacts contained within the neural recording data. The 16 microelectrode array signals, along with recorded cardiovascular indices (ECG, right atrium electrogram and haemodynamic data), were digitized via a Cambridge Electronics Design (Cambridge, UK; model 1401) data acquisition system for off-line analysis. The sampling frequency for neuronal data was 5.26 kHz; it was six times lower (0.877 kHz) for all other signals.

Cardiac and vascular mechanical stimuli

In order to determine whether identified right atrial neuronal populations transduce mechanosensory inputs from select cardiac tissues, the right ventricular conus and the left ventricular lateral wall were sequentially touched gently by a finger during 10 s intervals with at least 2 min baseline data obtained between stimulus applications. A length of saline-soaked umbilical tape was placed around the base of the inferior vena cava and another one around the descending thoracic aorta. Silk ligatures were placed around the left anterior descending coronary artery about 1 cm from its origin. This enabled us to repeatedly occlude the inferior vena cava (for 20 s), the descending aorta (for 20 s) and the left anterior descending coronary artery (for 1 min) while recording evoked changes in IC neuronal activities. At least 5 min separated each of these stressors, thereby allowing for return to basal activities.

Extracardiac efferent neuronal inputs

The left and right cervical vagosympathetic complexes and stellate ganglia were exposed. Bipolar electrodes were placed around each of them. Thereafter, these neural structures were stimulated individually via a Grass Model S88 Stimulator (Grass Co., Warwick, RI, USA). To establish the threshold for vagal efferent activation, the stimulus frequency was initially set to 20 Hz, pulse width to 2 ms and voltage increased until heart rate decreased by 10%. To establish the threshold for sympathetic efferent activation, frequency was set to 4 Hz, pulse width to 2 ms, with the threshold defined as the voltage necessary to increase heart rate or left ventricle (LV) dP/dt (first derivative (+ positive, – negative) of LV pressure) by

10%. During the course of each experiment, these efferent neural stimuli (right or left cervical vagosympathetic complex: RCV or LCV; right or left stellate ganglion stimulation: RSS or LSS) were periodically delivered for 1 min at 1 Hz, 2 ms pulse width, with stimulus voltages being $3 \times$ threshold. This was done to identify potential direct *versus* indirect inputs to IC neurons.

Mediastinal nerve stimulation

The right-sided mediastinal nerves that coursed over the ventral and ventro-lateral surfaces of the intrapericardial aspects of the superior vena cava were identified visually. In order to consistently elicit brief episodes of atrial arrhythmias, one or more of these mediastinal nerve sites were stimulated repeatedly via a bipolar electrode (inter-electrode distance 1.5 mm), as performed previously (Armour *et al.* 2005; Richer *et al.* 2008). Each active site was marked with India ink for identification during subsequent stimulations. The stimulator was controlled externally by the Cambridge Electronics Design data acquisition system running Spike2 software, with the macro for D/A output triggered by on-line atrial wave-front detection. Trains of five electrical stimuli (1–2 mA, 1 ms duration, and 5 ms pulse interval) were delivered for up to 20 s to each selected mediastinal site during the refractory period of each atrial beat. Contact between the bipolar electrode and the tissue was discontinued immediately after the onset of the atrial tachyarrhythmia.

Data analysis: signal processing of recorded multi-unit IC neuronal activity

Recorded neuronal activity generated by individual neuronal somata located throughout the RAGP was recorded, as described above. Recorded neuronal signals were contaminated by the electrical activity arising from the adjacent atrial myocardium located below the RAGP. Electrical artifacts induced during electrical stimulation of autonomic neural structures or mediastinal nerves could also be identified in the recorded signals. Artifact removal was thus necessitated, using the software Spike2 program (Cambridge Electronic Design). Four channels with neuronal activity were selected by visual inspection from all 16 channels of information. Simultaneously occurring activity displaying similar waveforms in each of three adjacent channels was interpreted as being artifactual as, for instance, representative of electrical activity generated by the adjacent atrial tissue. As such, these artifacts were identified using the template-matching functionalities of Spike2. The right atrial electrogram channel and the stimulator signal served to validate such artifact identification. In this manner, artifact wave-

forms were eliminated from all 16 channels. Figure 1 illustrates such an analysis process. These blanking intervals represented only 3% of the signal durations during sinus rhythm and up to 18% of signal duration during AF.

Following artifact removal, the activity generated by individual IC neuronal somata could be characterized by their specific amplitudes and waveforms derived from each of the 16 recorded linear microarray (LMA) channels. These signals were processed by analysing the activities recorded from pairs of adjacent electrodes (stereotrode). An action potential was considered to arise from a single IC neuronal somata and/or dendrites when two (but not more) adjacent electrodes displayed similar waveforms that occurred simultaneously in two adjacent electrodes. Action potentials derived from a single electrode were consistent with the waveforms observed from adjacent (but not distant) electrodes, this association remaining unchanging over time. Automatic waveform classification (i.e. identifying all the action potentials corresponding to the same IC neuron) was performed by template matching (template length: 5–6 ms, ~ 30 samples) and validated by principal component analysis. Further manual validation was performed by visual inspection of the templates such that artifact-related templates could be eliminated. Two similar templates (as established by principal component analysis) were merged when evidence arose (e.g. complementary intermittent firing) that the two firing time series so identified corresponded to a single neuron. Using that procedure, consistent waveforms derived from individual somata could be identified *in situ*, as has been done previously using a single unipolar electrode (Gagliardi *et al.* 1988; Ardell *et al.* 1991, 2009). Figure 1 illustrates this process to identify the activities generated by two separate IC neurons, as recorded concurrently from adjacent channels of the LMA electrode. Using these techniques and criteria, action potentials generated by individual somata and/or dendrites (not axons of passage) could be identified for up to 8 h (Ardell *et al.* 1991, 2009). At the completion of neural recording, animals were humanely killed under deep anaesthesia (50 mg kg^{-1} α -chloralose) using DC current-induced ventricular fibrillation.

Data analysis: monitoring individual neuron activity

Neuronal activity was compared in different time windows (before *versus* during an intervention such as touch or autonomic efferent nerve stimulation) by calculating the evolution of average neuronal activity rate. The time window before an intervention (baseline) was assessed for 1 min time periods. The time window during an intervention covered the actual duration of that intervention. The significance level of the observed differences in firing rate was assessed using a statistical test developed for

cortical neurons and based on the Skellam distribution (Shin *et al.* 2010) (see Appendix 1 for a detailed description of this analysis). The resulting P value was a function of the duration of the two time windows that were compared as well as the number of action potentials identified in each time window. Two levels of significance were employed: $0.01 < P < 0.05$ (moderate change) and $P < 0.01$ (strong change). Figure 2 illustrates such an analysis for baseline activity intervals of 60 s contrasted with stressor-evoked intervals of 60 s (panel A) or 5 s (panel B). Using this statistical approach, changes in action potential generation rates recorded before and during each intervention (e.g. afferent activation, stimulation of efferent inputs to IC network) were quantitatively evaluated for all identified IC neurons for each stressor.

Data analysis: conditional probability

This type of analysis quantifies whether a neuron that responded to one stressor also responds to another stressor. For that purpose, a neuron was said to respond to a stressor when a significant change in its activity rate ($P < 0.05$; either an increase or a decrease) was observed before and during each intervention (see above

and Fig. 2). The potential for a functional relationship between stressors X and Y was quantified within neurons identified in each dog as a conditional probability that a neuron that responded to stressor Y also responded to a stressor X. The conditional probability (Prob: response to Y | response to X) was estimated as the number of neurons that responded to both X and Y, divided by the number of neurons that responded to X.

Data analysis: χ^2

χ^2 analysis was used to compare potential interrelations between response characteristics of IC activity (e.g. basal activity with or without cardiac-related periodicity) and corresponding activity effects evoked by activation of specific afferent and efferent pathways.

Results

Spontaneous activity in physiological states

In the eight anaesthetized animals investigated, the activities generated by a total of 92 neuronal somata and/or dendrites (referred to as IC neurons hereafter) located

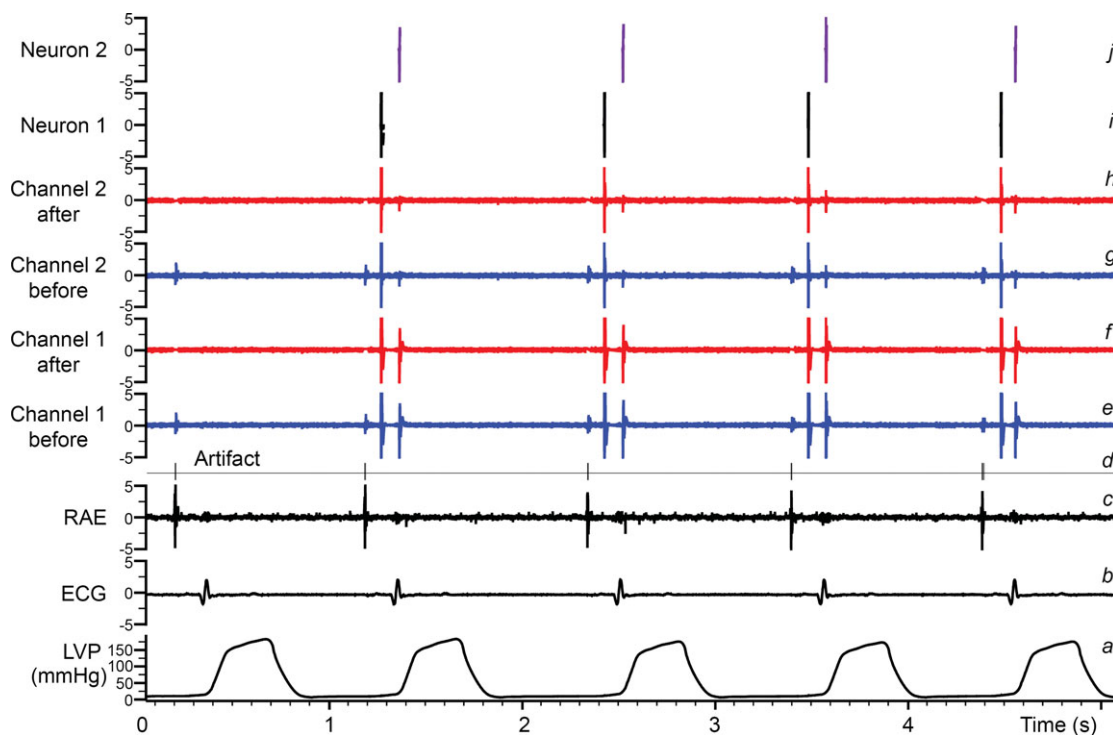


Figure 1. Methodology for the identification of individual IC neurons

Traces indicate: a, left ventricular chamber pressure (LVP); b, electrocardiogram (ECG); c, right atrial electrogram (RAE); d, event channel created from identified electrical/mechanical artifacts; e and g, raw signal recordings of two channels from the multichannel linear microarray electrode; f and h, neuronal recordings from channels e and g after artifact removal based on the event channel d; i and j, two final neuronal waveforms extracted from a stereotrode built from channels f and h using principal component analysis. These final waveforms (i and j) represent basal activity from two separate IC neurons located within the right atrial ganglionated plexus; such activity can be evaluated continuously and concurrently for hours and in response to imposed stressors.

at different depths (superficial, intermediate and deep) within the RAGP were identified using the LMA electrode (average: 11.5 neurons per dog). The spontaneous activity generated by each was assessed by pooling the data from the 1 min time interval baselines obtained before each of the ten interventions. Spontaneous spiking activity varied considerably among neurons. As shown in Fig. 3, baseline firing frequency ranged from 0 to 2.7 Hz, 68% being <0.1 Hz and 8% being >0.4 Hz. Although 12% of these neurons were never active during the 1 min intervals immediately before the interventions commenced, all of these became active at some time during or after one or more of the interventions.

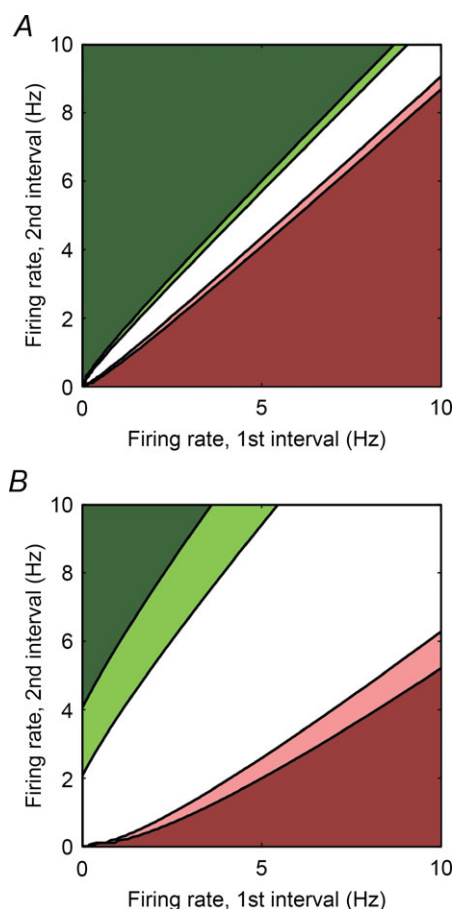


Figure 2. Quantitative assessment of significance (P values) when comparing the firing rate in two intervals: baseline to stress-evoked response

P values are computed using the Skellam test and displayed as a function of the average firing rate in the first and in the second interval. The dark red and light red colours mean that the firing rate is strongly ($P < 0.01$) or moderately decreasing ($0.01 < P < 0.05$), respectively. The dark green and light green colours mean that the firing rate is strongly ($P < 0.01$) or moderately increasing ($0.01 < P < 0.05$), respectively. *A*, both intervals last 60 s (baseline interval 1 and response during stressor interval 2). *B*, the first interval (baseline) has a duration of 60 s and the second (response during stressor) has a duration of 5 s.

Within these control intervals, some neurons (43 of 92) generated spikes that clustered around specific phases of the cardiac cycle. Figure 4 illustrates this relationship such that neuron 1 was preferentially active during the left ventricular ejection phase and another neuron (neuron 2) was preferentially active during left ventricular isovolumetric contraction. Other identified neurons (e.g. Fig. 4, neuron 3) generated activity patterns that did not relate to a specific phase of the cardiac cycle. Using spike-triggered averaging, it was possible to demonstrate the temporal correlation between some IC neurons thereby indicating interdependent relationships within IC networks. Figure 5 demonstrates such a relationship for two IC neurons that generated activities with cardiac-related periodicity. For instance, the activity generated by neuron 1 was, on average, followed within a few milliseconds by activity generated by neuron 2. Note that this interdependent relationship was dynamic in nature such that they displayed interspike intervals that varied over time in the temporal relationship of their activities to each other (minimum 8 ms; peak of the histogram at 12 ms, see Fig. 5C) and that furthermore the activities displayed by these two neurons were not always coupled during every cardiac cycle.

Cardiovascular mechanoreceptor activation evoked IC responses

Within identified populations of IC neurons of the RAGP, 22% responded significantly to touching the ventricular epicardial surface in one or more regions (right ventricle (RV) conus, RV sinus or ventral LV). A typical neuronal response to touch is shown in Fig. 6. In this example, during touch, the activity generated by two neurons became inhibited, while others were activated. Note that some other neurons (e.g. neuron 8) were relatively unaffected by this gentle epicardial touch. The significance of changes induced in the activity rates of each of the identified neurons in each of the dogs during each of the stressors studied is summarized in Fig. 7 and Table 1.

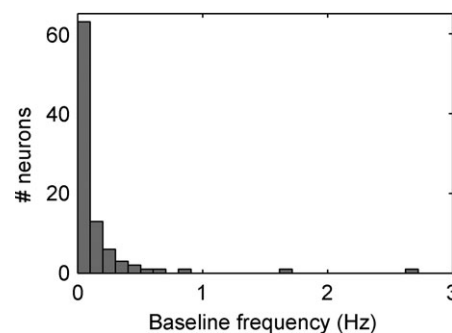


Figure 3. Histogram of baseline frequencies of all identified IC neurons

Note that even within a given animal, a common stressor (e.g. touch of RV or LV) can evoke differential neuronal effects, even from closely adjacent IC neurons. For instance, of IC neurons modulated by ventricular touch, activity generated by 76% (16 of 21) increased while that of 24% (5 of 21) decreased (Table 1).

The activities generated by 41% (38 of 92) of identified IC neurons changed when the inferior vena cava (IVC) or the descending thoracic aorta was occluded briefly; of these, 39% were affected by both stressors (15 of 38). As indicated in Table 1, IC activity was either increased ($n=37$) or decreased ($n=16$) among these differing neuronal populations in response to one stressor, even within a given animal (Fig. 7). In the case of ventricular touch and occlusion of the great vessels, IC neurons generating lower level basal activity tended to be activated by these stressors while the activities of those with higher levels of basal activity tended to be suppressed by these same stressors (Table 1). Overall, 50% of recorded IC

neurons (46 of 92) were modified by ventricular touch or occlusion of the great vessels.

Evoked IC response to stimulation of central inputs

Previous studies using a single unipolar electrode found that few RAGP neurons received direct inputs from medullary (parasympathetic efferent preganglionic) neurons or stellate ganglia neurons, as determined by fixed latency evoked responses between RAGP neuronal activity and individual electrical stimuli applied at low frequencies to a stellate ganglion or a cervical vagus nerve (Gagliardi *et al.* 1988). Based upon these fixed latency criteria, none of the 92 RAGP neurons evaluated in this study received direct central neuronal inputs. On the other hand, the activity of 42% (39/92) of identified IC neurons was modified in response to 1 Hz stimulation of either stellate ganglion, indicating

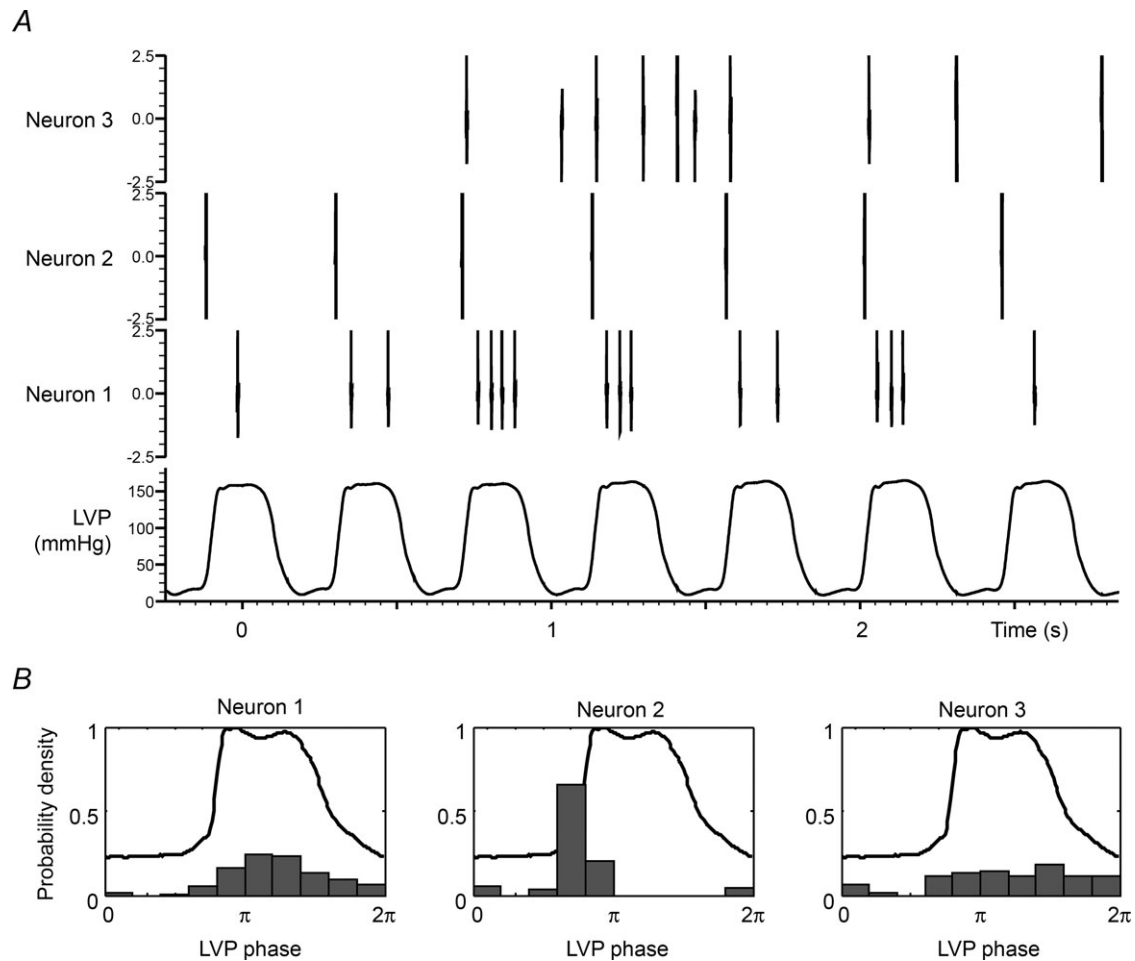


Figure 4. Subpopulations of IC neurons demonstrate cardiac-related neuronal activity

A, LV pressure and representative examples of neurons that are primarily active during left ventricular ejection (neuron 1), during isovolumetric contraction phase for LV (neuron 2) or with activity independent of LVP (neuron 3). B, for each of these neurons, the probability density of firing as a function of the position within the LVP cycle (expressed as a phase between 0 and 2π) is indicated along with the average LVP profile.

indirect input activation of such neurons with non-fixed latencies (Fig. 7 and Table 1). Of these IC neurons, 10 were influenced by RSS alone, 12 by LSS alone and 17 others were affected by both of these central neuro-

nal inputs. The predominant effect of stellate stimulation on IC activity was excitation (Table 1). Likewise, when low frequency electrical stimuli (1 Hz) were applied to either cervical vagus, the IC activity from 41% (38/92) of

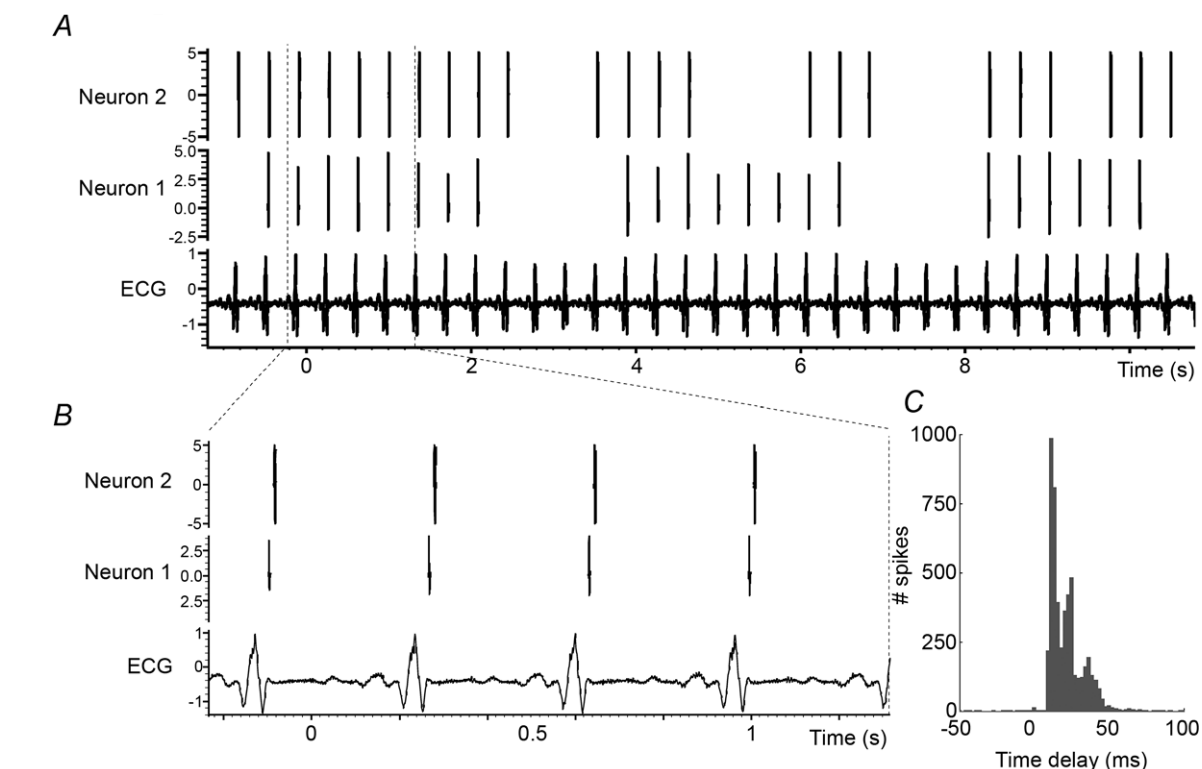


Figure 5. Long-term interdependent activity of two IC cardiovascular-related neurons

A, ECG and concurrent spontaneous activity of two IC neurons. B, zoom of A over 4 cardiac cycles. C, spike-triggered (neuron 1 to neuron 2) histogram of spontaneous activity for these two IC neurons recorded over 2 h. Note maintained temporal relationship, but with some variation in such interdependent activity.

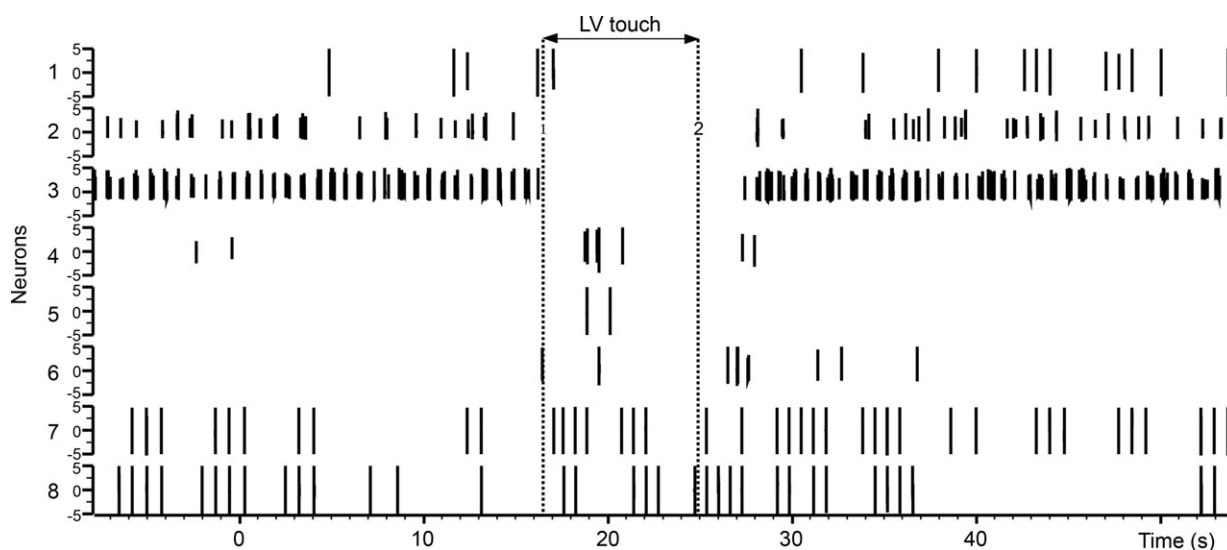


Figure 6. Left ventricular touch differentially modifies IC activity

The spiking activities concurrently recorded from 8 selected IC neurons in a single animal are shown. Vertical dotted lines indicate onset and offset of touch. Note that subpopulations of IC neurons show diminished activity during touch (e.g. neurons 2 and 3), some are activated by touch (e.g. neuron 7) and some are unaffected (e.g. neuron 8).

identified neurons was modified – doing so after non-fixed latencies (Fig. 7 and Table 1). Of these IC neurons, 17 were impacted by RCV alone, 7 by LCV alone and 14 by both vagi. The predominant effect of vagal stimuli on affected IC neurons was excitatory in nature (Table 1). At 1 Hz

stimulation frequencies, induced changes in LV systolic pressure or LV $-dP/dt$ were less than 5% of baseline in response to either cervical vagal or stellate stimulation indicating minimal evoked changes in cardiac inotropic function. While induced chronotropic responses to 1 Hz

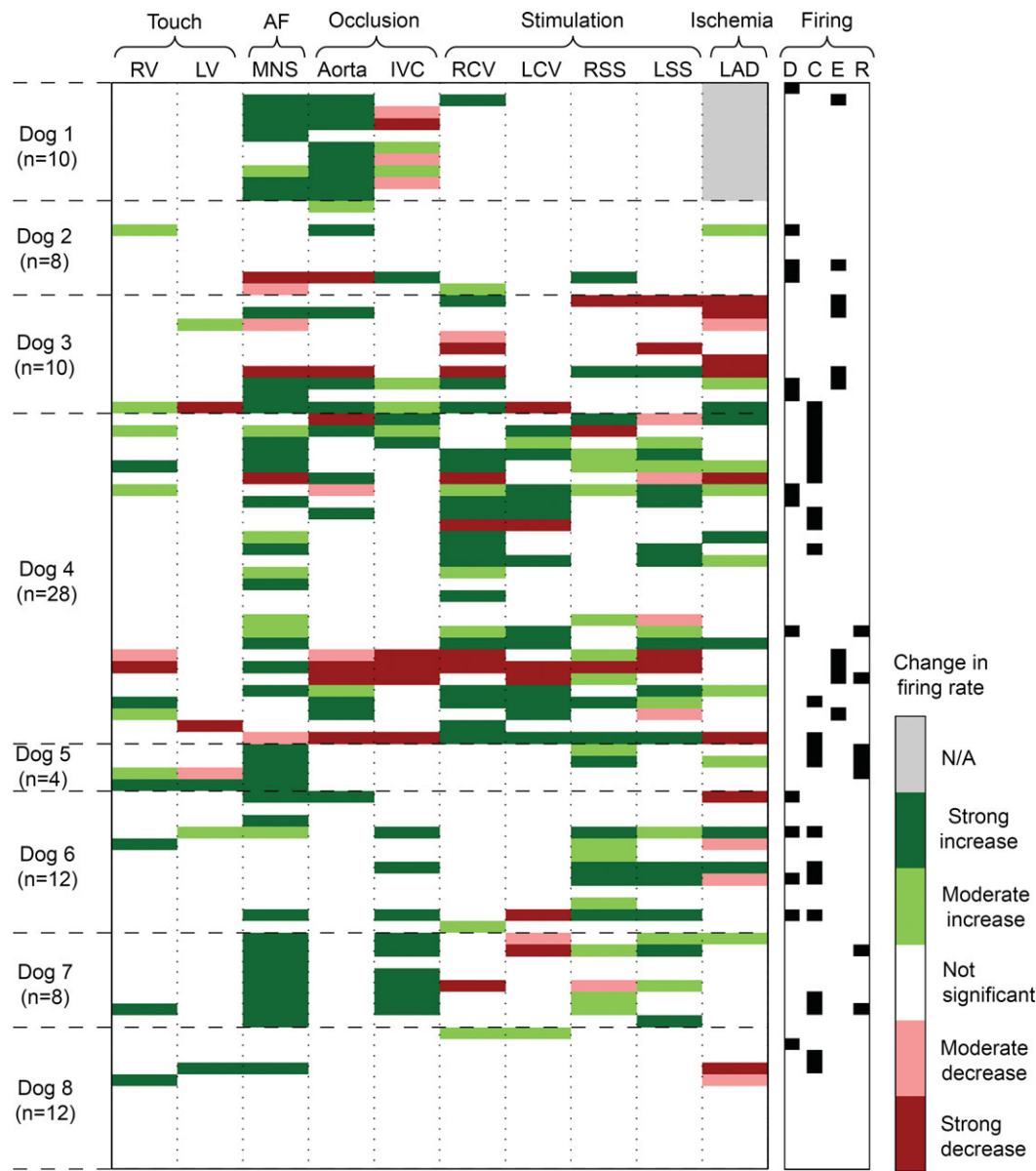


Figure 7. Varied responses displayed by each neuron studied in response to differing sensory or central efferent neuronal stressors
Each horizontal column represents how each identified right atrial neuron in all 8 dogs responded to each of the stressors applied (horizontal row above). Each column is associated with a specific stressor: afferent activation (touch of right (RV) or left (LV) ventricle; occlusion of inferior vena cava (IVC) or descending aorta; myocardial ischaemia evoked by transient occlusion of left anterior descending coronary artery (LAD)), activation of efferent inputs to the RAGP via electrical stimulation of the right (RCV) or left (LCV) cervical vagus or stellate ganglia (right, RSS; left, LSS), or global activation of the IC network evoked by electrical stimulation of mediastinal nerves (MNS) at levels sufficient to evoke atrial fibrillation (AF). The number (n) of neurons so identified in each animal is indicated to left. The significance of each change ranged from greatest ($P < 0.01$) to moderate ($0.01 < P < 0.05$) to insignificant (N/A; grey bar means that an intervention was not performed). Right-hand column characterized whether neuron CV-related activity occurred during diastole (D), isovolumetric contraction (C), LV ejection (E) or isovolumetric relaxation (R).

Table 1. Evoked changes in IC activity in response to afferent and efferent stressors

Stressor	Increased FF ($P < 0.01$)				Increased FF ($P < 0.05$)			
	Baseline	Stress	P value	n	Baseline	Stress	P value	n
RV	0.01 \pm 0.01	0.42 \pm 0.19	$P = 0.03$	6	0.03 \pm 0.05	0.44 \pm 0.28	$P = 0.00$	12
LV	0.25 \pm 0.02	0.91 \pm 0.19	$P = 0.50$	2	0.15 \pm 0.12	0.64 \pm 0.33	$P = 0.12$	4
Ao Occl	0.05 \pm 0.08	0.98 \pm 1.03	$P = 0.00$	18	0.04 \pm 0.08	0.89 \pm 1.01	$P = 0.00$	20
IVC Occl	0.12 \pm 0.27	0.59 \pm 0.87	$P = 0.00$	12	0.09 \pm 0.23	0.46 \pm 0.75	$P = 0.00$	17
RCV	0.06 \pm 0.10	0.73 \pm 0.56	$P = 0.00$	17	0.05 \pm 0.09	0.57 \pm 0.56	$P = 0.00$	23
LCV	0.13 \pm 0.24	0.57 \pm 0.58	$P = 0.00$	12	0.11 \pm 0.22	0.51 \pm 0.56	$P = 0.00$	14
RSS	0.14 \pm 0.13	0.71 \pm 0.45	$P = 0.00$	10	0.15 \pm 0.30	0.48 \pm 0.50	$P = 0.00$	23
LSS	0.16 \pm 0.17	0.66 \pm 0.37	$P = 0.00$	14	0.19 \pm 0.20	0.60 \pm 0.36	$P = 0.00$	21
MNS	0.18 \pm 0.90	1.43 \pm 1.90	$P = 0.00$	35	0.15 \pm 0.82	1.24 \pm 1.79	$P = 0.00$	42
LAD CAO	0.18 \pm 0.12	0.78 \pm 0.75	$P = 0.03$	6	0.26 \pm 0.23	0.66 \pm 0.56	$P = 0.00$	14
Stressor	Decreased FF ($P < 0.01$)				Decreased FF ($P < 0.05$)			
	Baseline	Stress	P value	n	Baseline	Stress	P value	n
RV	4.03 \pm 0.00	0.12 \pm 0.00	$P = 1.00$	1	2.67 \pm 1.92	0.12 \pm 0.00	$P = 0.50$	2
LV	0.70 \pm 0.52	0.26 \pm 0.04	$P = 0.50$	2	0.67 \pm 0.37	0.22 \pm 0.08	$P = 0.25$	3
Ao Occl	1.54 \pm 0.93	0.51 \pm 0.63	$P = 0.03$	6	1.33 \pm 0.89	0.44 \pm 0.57	$P = 0.01$	8
IVC Occl	1.19 \pm 1.39	0.12 \pm 0.15	$P = 0.06$	5	0.79 \pm 1.18	0.08 \pm 0.13	$P = 0.01$	8
RCV	0.74 \pm 0.53	0.15 \pm 0.19	$P = 0.02$	7	0.67 \pm 0.53	0.14 \pm 0.18	$P = 0.01$	8
LCV	0.51 \pm 0.40	0.12 \pm 0.16	$P = 0.03$	6	0.53 \pm 0.37	0.15 \pm 0.18	$P = 0.02$	7
RSS	2.00 \pm 2.44	1.29 \pm 2.17	$P = 0.25$	3	1.53 \pm 2.20	0.97 \pm 1.88	$P = 0.12$	4
LSS	1.54 \pm 1.43	0.48 \pm 0.55	$P = .12$	4	1.00 \pm 1.13	0.37 \pm 0.43	$P = 0.01$	8
MNS	0.79 \pm 0.21	0.08 \pm 0.10	$P = .25$	3	0.51 \pm 0.35	0.07 \pm 0.09	$P = 0.03$	6
LAD CAO	0.64 \pm 0.54	0.17 \pm 0.29	$P = 0.01$	8	0.48 \pm 0.49	0.13 \pm 0.24	$P = 0.00$	12

IC neuronal activity (mean \pm SD) at baseline and in response to indicated stressors (see Abbreviations). Responses are subdivided based upon evoked increases in activity (upper rows) and decreased activity (lower rows). P values were derived based on analysis described in Appendix and Fig. 2. Based on that analysis, responses are subdivided based upon evoked responses with $P < 0.01$ (left panels) and $P < 0.05$ (right panels). FF, firing frequency; Ao, aortic; Occl, occlusion.

vagal nerve stimulation showed less than 5% difference from baseline ($P = 0.94$), LSS increased heart rate on average from 96.6 ± 11.9 to 103.2 ± 10.1 beats min^{-1} ($P = 0.30$) and RSS from 101.1 ± 12.6 beats min^{-1} baseline to 120.2 ± 0.3 beats min^{-1} ($P < 0.01$).

Some IC neurons received convergent inputs from both efferent limbs of the autonomic nervous system. Fifty-six percent (52/92) of identified IC neurons responded to some combination of cervical vagal nerve (RCV, LCV) or stellate ganglia (RSS, LSS) nerve stimulation. Of these 52 IC responders, 5 were activated by all 4 inputs, 12 were activated by 3 of 4 inputs, 17 responded to 2 inputs and 18 responded solely to 1 input. Overall, 48% (25/52) evoked a response to both vagal and sympathetic inputs, 25% (13/52) responded solely to vagal (RCV or LCV) stimulation and the remaining 27% (14/52) responded solely to central sympathetic (RSS or LSS) efferent neuronal inputs.

Cardiac-related IC periodicity: relationship to afferent and efferent inputs

Figure 8 shows activity histograms obtained for all IC neurons that generated at least 100 action potentials

during baseline recording periods. Of the 49 neurons so identified, 43 generated activity that clustered around specific phases of the cardiac cycle. The majority of that cardiac periodicity was evident during diastole (14 neurons) or isovolumetric contraction (22 neurons), with lesser aggregate activity being evident in the ejection phase (10 neurons) or during isovolumetric contraction (7 neurons). Twenty-three per cent of IC neurons with cardiac-related periodicity exhibited dual activity peaks in relationship to LV pressure during the cardiac cycle.

Figures 7 and 9 demonstrate the differential effects of afferent and efferent inputs on IC activity from neurons that displayed cardiac-related periodicity *versus* those that did not. Following χ^2 analysis of the neuronal data, it is evident that those IC neurons that generated cardiac-related activities were preferentially modified by mechano-sensitive inputs (RV touch, LV touch, aortic occlusion or IVC occlusion) as well as by activation of each of the primary central efferent neuronal inputs to the IC network, both sympathetic (stellate stimulation) and parasympathetic (vagal stimulation) in origin. In contrast, transient occlusion of the left anterior descending coronary artery (LAD) evoked similar changes in the activity of neurons, whether they did or did not display cardiac-related periodicity during basal states.

LV ischaemia and evoked IC responses

Myocardial ischaemia induced by transient LAD occlusion triggered a response in 32% (26/82) of identified IC neurons. Transient myocardial ischaemia increased activity in 14 of these neurons and depressed that of 12 neurons (Table 1). Such activity changes were manifest during ischaemia and during early reperfusion. Figure 10 (top panel) summarizes the corresponding sensitivity to activation by cardiac mechano-sensitive inputs (RV touch, LV touch, aortic occlusion and IVC occlusion) in IC neurons that responded to LAD occlusion compared to IC neurons that were ischaemia insensitive. χ^2 analysis indicated that ventricular ischaemia-sensitive IC neurons also displayed increased responsiveness to cardiac afferent inputs. In contrast, responsiveness to either vagal or stellate stimulation was similar between ischaemia-sensitive *versus* -insensitive IC neurons (Fig. 7 and χ^2 analysis with P greater than 0.05).

Atrial arrhythmia induction

Short episodes of atrial arrhythmia (duration ~20 s) were initiated repeatedly when brief bursts of electrical current were delivered to selected right-sided mediastinal nerves during the atrial refractory period. Arrhythmia induction via mediastinal nerve stimulation (MNS) was the stressor, by itself, that affected the largest number of identified neurons (Table 1: 48 of 92 neurons). Of those IC neurons affected by MNS, 88% (42 of 48) increased their activity and 12% (6 of 48) exhibited reduced activity during AF (Table 1 and Fig. 7). χ^2 analysis also indicated that the sensitivity of IC neurons that responded to mediastinal nerve stimulation was reflective of an increased responsiveness to cardiac afferent inputs (Fig. 10, bottom panel). In contrast, IC responsiveness to either vagal or stellate ganglion inputs was similar when comparing MNS-sensitive *versus* MNS-insensitive neurons (Fig. 7 and χ^2 analysis with P greater than 0.05).

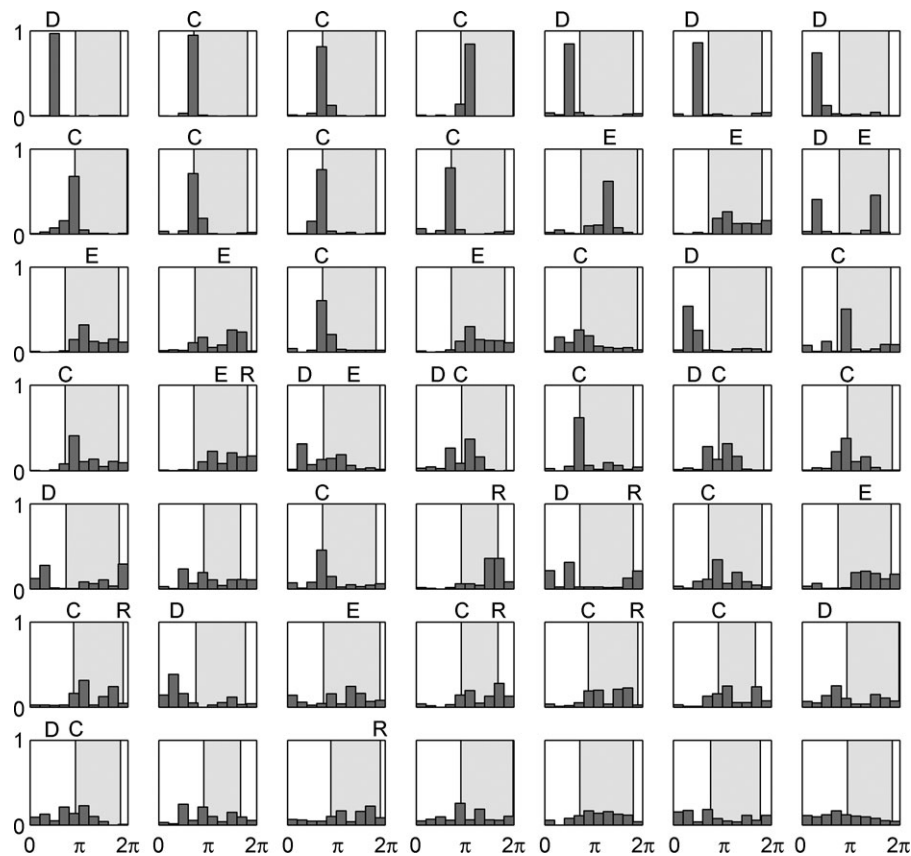


Figure 8. IC neurons with cardiac-related activity are preferentially active during diastole to isovolumetric contraction phases

Activity histograms for all identified IC neurons that generated at least 100 spikes at baseline (49 of 92). Shaded area indicates time of LV contractile phase. The activities of these IC neurons are sorted according to entropy of distribution. Classification of firing patterns, relative to cardiac cycle, indicated above each neuron based upon bin (or immediately adjacent bin) counts that exceed 30% of total activity. Distribution of firing was: 14 neurons active in diastole (D), 22 neurons active during isovolumetric contraction (C), 10 neurons active during ejection phase (E), 7 units active during isovolumetric relaxation (R). Ten neurons showed dual peaks. Six neurons that exhibit adequate basal activity failed to demonstrate cardiac-related periodicity in firing.

Interdependence of neuronal function in response to different stressors

Figure 11A summarizes, in matrix format, the relationships of the various identified IC neurons when comparing their responses to all 10 stressors tested. It was found that all 10 of these conditional probabilities (CPs) generated specific neuronal relationships. As such, their corresponding ($CP \geq 0.6$) functional interconnectivities can be represented as a network (cf. Fig. 11B). These relations so displayed do not necessarily imply a mechanistic link between neurons initiated by these stressors. Rather, these relationships appear to reflect the concordant behaviour among RAGP neuronal populations induced by pairs of independent stressors. Note that conditional probability links responses initiated among afferent stressors (e.g. IVC and aortic occlusion) in contrast to those initiated by differential central efferent neuronal inputs to the IC network (RCV, LCV, RSS and LSS). Furthermore, these data indicate a convergence point of the IC neuronal population that transduces both afferent and efferent inputs – a local circuit neuronal population engaged by MNS in the induction of atrial arrhythmias.

Discussion

Neural control of the heart depends upon the dynamic interplay between a series of nested feedback loops involving peripheral and central aspects of the cardiac nervous system (Zucker & Gilmore, 1991; Armour, 2008). The intrinsic cardiac nervous system (ICNS) represents the most distal of its control loops and, as such, functions as the final common pathway for cardiac control (Ardell *et al.* 1991, 2004; Armour, 2008). The data derived from the experiments reported here demonstrate the primary inherent characteristics of the major neuronal subpopulations within the ICNS, including the fact that the integrative characteristics of its different local circuit neuronal populations differ in the transduction of specific cardiac afferent- or central efferent-derived neuronal inputs.

The majority of intrinsic cardiac (IC) neurons that were functionally identified in this study exhibited low levels of spontaneous activity in control states, 68% exhibiting a basal activity of less than 0.1 Hz. The data derived from this study further demonstrate the state dependence of the majority of these intrinsic cardiac neurons that predicated their response characteristics to select

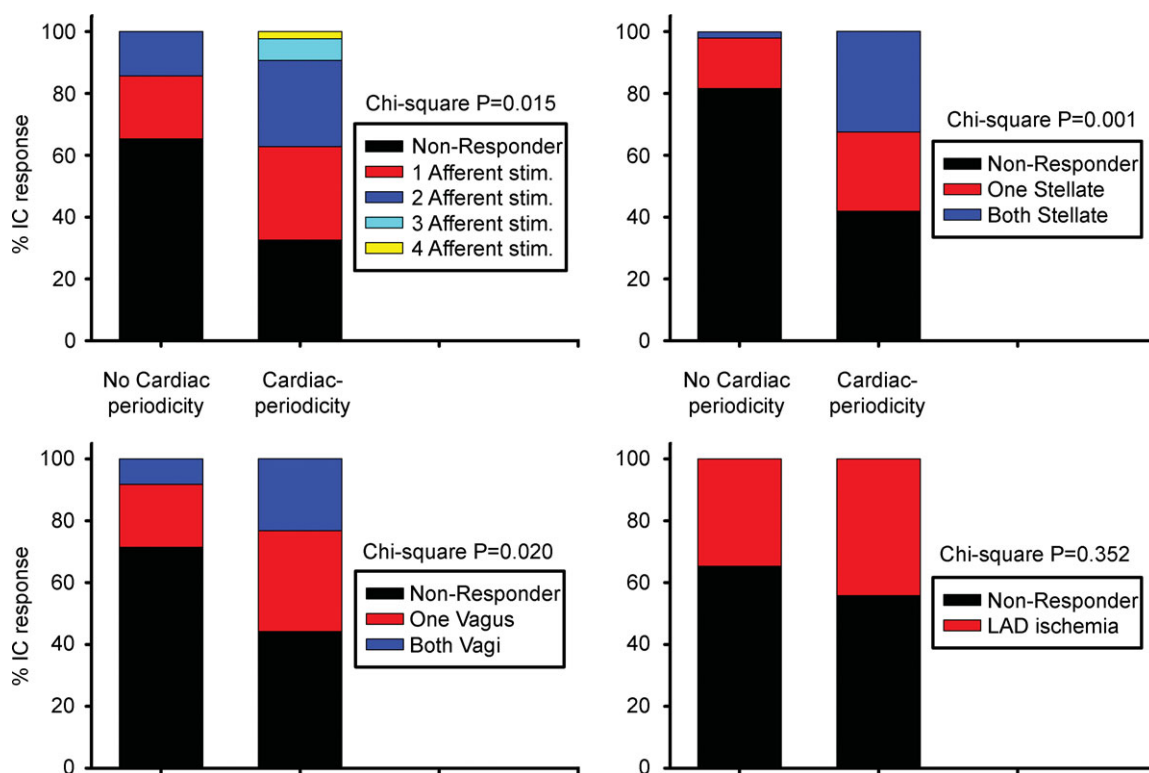


Figure 9. IC neurons displaying cardiac-related activity are modified differentially by afferent and efferent stressors

Proportion (% responders) of IC neurons with basal cardiac (cardiac periodicity) vs. non-cardiac cycle (no cardiac periodicity)-related periodicities whose activity was modified by afferent neuronal inputs (top left panel: RV touch, LV touch, transient occlusion of IVC or descending aorta), efferent neuronal inputs (top right panel, stellate ganglia; bottom left panel, cervical vagi) or transient occlusion of the LAD (bottom right panel). χ^2 P values are indicated for each subclass of stressor.

cardiovascular stressors (Kember *et al.* 2001; Waldmann *et al.* 2006). For example, the baseline activity displayed by many IC neurons appeared to determine how such neurons responded to specific afferent *versus* efferent neuronal inputs to the ICNS. Those IC neurons exhibiting low basal firing levels in control states were for the most part activated by cardiovascular stressors, while those exhibiting higher basal firing rates tended to be suppressed by cardiovascular stressors.

Fundamental to our understanding of control of regional cardiac indices, the various subsets of IC neurons identified in this study demonstrated interdependent neuronal behaviour, even during basal states. Previous work from our laboratory has suggested that such neuronal activity interdependence is indicative of common shared cardiopulmonary afferent inputs to the ICNS, ones that primarily rely upon functional interconnectivity mediated via (i) local network interactions and (ii) divergent descending projections from higher centres to the distributive IC networks (Armour *et al.* 1998; Thompson *et al.* 2000; Randall *et al.* 2003; Waldmann *et al.* 2006). As such, we have proposed that this overlapping control system allows for effective local reflex modulation of regional cardiac electrical and mechanical indices while,

at the same time, providing a peripheral substrate for higher centres to impact cardiac function (Ardell, 2004; Armour, 2008).

The intrinsic cardiac nervous system is a distributed neural network capable of independent and inter-dependent reflex processing of cardiac sensory and central neuronal inputs (Ardell *et al.* 1991; Thompson *et al.* 2000; Waldmann *et al.* 2006). While efferent postganglionic neuronal outputs to the target organ arising from the various aggregates of intrinsic cardiac ganglia exert preferential control over different regions of the heart, many exert modulating effects over divergent cardiac regions because of ICNS interconnectivity (e.g. RAGP neurons evaluated in this report are primarily associated with control of atrial function; Ardell & Randall, 1986; Yuan *et al.* 1994; Gray *et al.* 2004a). Thus, changes can occur in the function of neurons located in multiple sites throughout the intrinsic cardiac nervous system in response to activation of select populations throughout the intrinsic cardiac ganglionated plexus (Yuan *et al.* 1993; Cardinal *et al.* 2009). This distribution/cascade of IC control ultimately results in a combined capacity to influence tissues throughout the atria and ventricles.

The intrinsic cardiac nervous system is composed of a heterogeneous population of neurons (Gagliardi *et al.* 1988; Adams & Cuevas, 2004; Parsons, 2004; McAllen *et al.* 2011). Prior neurophysiological studies using unipolar recording electrodes demonstrated that its neurons can be functionally subdivided into afferent, local circuit and efferent neurons, the latter involving both sympathetic and the expected parasympathetic post-ganglionic neurons (Ardell, 2004; Armour, 2008). Prior anatomical and immunohistochemistry approaches have supported this stratification in both humans and various animal models (Yuan *et al.* 1994; Armour *et al.* 1997; Parsons, 2004; Hoover *et al.* 2009). Utilizing classical neurophysiologically based definitions, afferent neurons would be defined as those transducing a circumscribed cardiac receptor field with preferential modality sensitivity (Brown, 1979; Zucker & Gilmore, 1991; Kember *et al.* 2001; Armour & Kember, 2004). Classically, autonomic efferent post-ganglionic neurons would be defined as those somata that can be activated monosynaptically following application of electrical stimuli to their pre-ganglionic neuronal inputs (cf. the vagi or stellate ganglia; Langley, 1921). The population of local circuit neurons (LCNs) would be the remainder of the neurons of the ICNS that receive (i) secondary inputs from the IC afferent/efferent subpopulations depicted above, in addition to (ii) inter-connecting inputs derived from other LCNs located in the same or other ganglia.

It has been proposed that the primary functions of the IC LCNs are to: (i) process and coordinate dynamic afferent and efferent derived inputs which, in turn, (ii) modulate efferent postganglionic neuronal outputs to

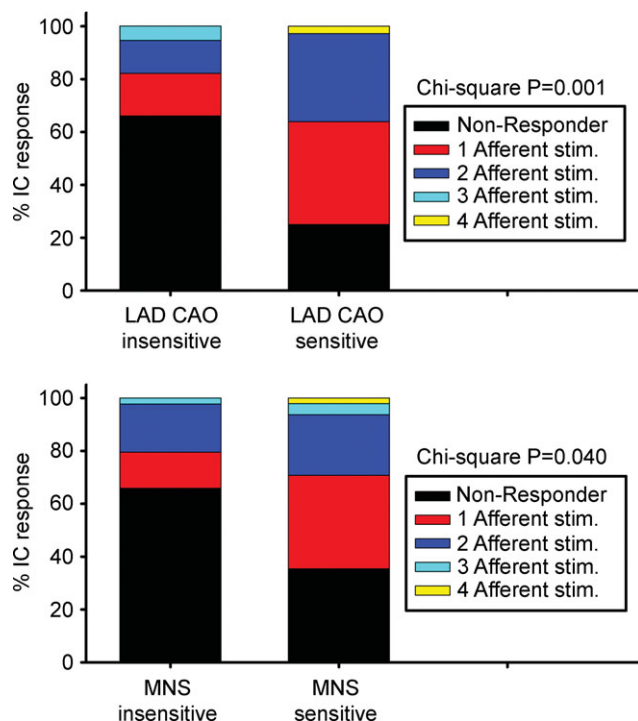


Figure 10. Afferent sensitivity to mechanical stressors predicts IC responsiveness to ischaemic or MNS stressors

Proportion of IC neurons modified by afferent stressors (RV touch, LV touch, transient occlusion of IVC or descending aorta) divided according to their sensitivity to transient LAD coronary artery occlusion (CAO; top panel) vs. mediastinal nerve stimulation (bottom panel). χ^2 P values are indicated for each subclass of stressor.

various cardiac regions (Ardell, 2004; Armour, 2008). Given these assumptions and, as summarized in Fig. 11, we now propose that LCN populations should be subdivided into three basic subclasses: (i) secondary afferent LCNs, (ii) secondary efferent LCNs, and (iii) the convergent LCNs. Each of these subpopulations exhibit preferential response characteristics to various stressors. For instance, secondary afferent LCNs transduced multiple and divergent cardio-pulmonary mechanical and chemical stressors in a secondary fashion. In like manner, the secondary efferent LCNs received multiple indirect (not mono-synaptic), but consistent, inputs from central sympathetic and/or parasympathetic efferent neuronal sources. Our data further indicate that many of these secondary afferent and efferent LCNs interconnect with other populations – the convergent LCNs. The convergent LCNs can be best represented by their collective responsiveness to excessive nerve input imbalances – as induced in this study by mediastinal nerve stimulation.

Central neuronal command

Central and peripheral aspects of the cardiac nervous system act synergistically to regulate regional cardiac function (Armour *et al.* 1998, 2008; Ardell, 2004; Herring

& Paterson, 2009; McAllen *et al.* 2011). Data derived from this study indicate that over half (56%) of IC neurons received indirect and frequently convergent central efferent neuronal inputs via the vagi and/or stellate ganglia. In accord with that finding, there was a substantial convergence of right- and left-sided autonomic efferent inputs onto identified IC neurons. For instance, of the 42% of the population that responded indirectly to sympathetic efferent neuronal inputs, 56% were modulated by unilateral inputs and 44% by inputs from both stellate ganglia. Correspondingly, of the 41% of IC neurons that responded to vagal nerve stimulation, 63% responded to unilateral inputs and 37% to bilateral inputs. The predominant effect of these central neuronal inputs to ICNS was excitatory in nature. Of those IC neurons responding to electrical stimulation of these preganglionic inputs, 25% responded solely to stellate stimulation and 25% responded solely to vagal activation; these neurons are defined as secondary efferent LCNs since they did not respond with fixed latencies in response to preganglionic efferent stimulation. The remaining 50% of IC neurons identified by autonomic stimulation responded to inputs from both central neuronal sources: at least one stellate ganglion and one cervical vagus; these neurons are defined as convergent LCNs. This latter population may subserve,

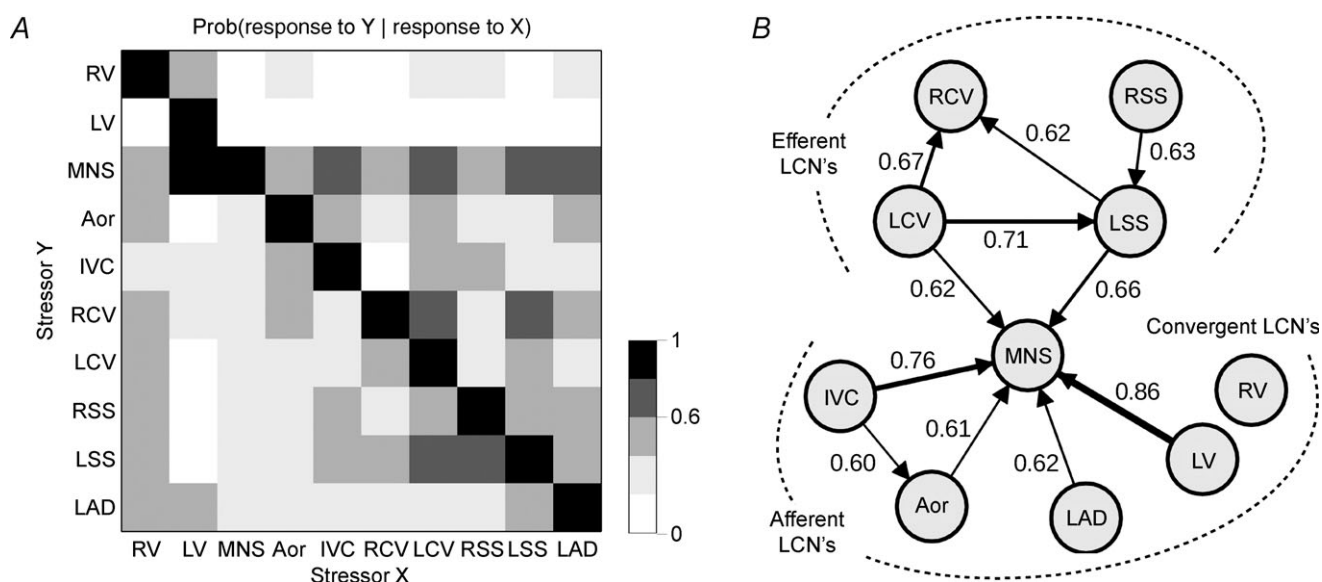


Figure 11. Interdependent activity among IC neurons in response to transient afferent or efferent stressors

A shows conditional probability that one neuron responding to one stressor (X, x-axis) responded to another stressor (Y, y-axis). Aor: aortic occlusion; other acronyms as in Fig. 7. Grey scale indicates level of probability of each occurrence (0–1 in 0.2 increments). B graphical representation of the pattern of interdependent interactions between applied stressors. Arrow thickness is proportional to the strength of conditional probability, whose value is also indicated next to each arrow. Only links with conditional probabilities ≥ 0.6 are displayed. Mediastinal nerve stimulation (MNS) is a pre-eminent stressor, evoking changes in 52% of recorded IC neurons (48 of 92). Interdependent interactions among the IC neurons in response to stressors fall into two principal categories: efferent dependent and afferent dependent; stressor-evoked activity in both subpopulations of IC neurons is similarly predictive of activation in response to MNS. Seventeen per cent of recorded IC neurons (16 of 92) were not significantly affected by any of the stressors applied.

in part, the role of sympathetic/parasympathetic interactive control of regional cardiac function, as occurs at ICNS sites separate from the end-effectors (Furukawa *et al.* 1996; McGuirt *et al.* 1997; Randall *et al.* 1998; Herring & Paterson, 2009).

Sensory neural inputs

For a given cardiovascular (CV) afferent stressor or combination of stressors, the evoked change in neuronal activity of a given responsive IC neuron was found to be reproducible. Few of these afferents could be classified as primary afferent neurons, i.e. those that responded to one modality arising from a restricted receptive field (Brown, 1979; Armour & Kember, 2004). Thus, the majority of the neurons so identified can be more appropriately classified as secondary afferent LCNs.

Secondary afferent LCNs transduce multimodal inputs from the great thoracic vessels and/or different regions of the heart. In fact, in some cases mechano-sensitive afferent inputs arising from these different cardiopulmonary regions evoked directionally differential responses in various IC neurons, even when studying the evoked activities generated by adjacent IC neurons. About 50% of the IC neurons that exhibited cardiac cycle-related periodicity displayed activity primarily during late diastole into isovolumetric contraction. Furthermore, those IC neurons that displayed cardiac cycle-related periodicity were found to preferentially transduce not only mechano-sensitive inputs but also descending central neuronal efferent inputs. This observation demonstrates the diverse nature of the processing capabilities of individual IC neurons. It also suggests an ability of the network to respond appropriately to multiple afferent inputs arising from different cardiac regions or from major vessels adjacent to the heart. All of which indicates that the afferent neuronal transduction capabilities of the ICNS may account for the fact that many of its neurons involved in the synchrony of regional cardiac contractile function display beat-to-beat activity patterns reflective of regional cardiodynamics (Armour *et al.* 1998, 2008).

It has been proposed that common shared CV afferent neuronal inputs can subserve a primary role in the interactive behaviour among neuronal somata in (i) the ICNS and (ii) extracardiac intrathoracic autonomic ganglia (including the mediastinal, middle cervical and stellate ganglia) in the determination of local network interactions (Armour *et al.* 1998; Kember *et al.* 2001; Armour & Kember, 2004; Waldmann *et al.* 2006). As such, these can be impacted by cardiovascular stressors, including: (1) asymmetric activation of extracardiac neuronal inputs into and between IC nerve networks in the induction of atrial arrhythmogenesis (Armour *et al.* 2005; Richer *et al.* 2008); and (2) ischaemia-induced excessive activation of

ventricular afferent neurons inducing heterogeneous and excessive activation of local circuit neurons (Huang *et al.* 1993; Armour *et al.* 1998; Waldmann *et al.* 2006). Such derangements of cardiac control networks can contribute to the potential for sudden cardiac death (Schwartz *et al.* 1992; Billman, 2006; Vanoli *et al.* 2008). Moreover, disruptions and remodelling of network interconnections within the cardiac nervous system, including its ICNS elements (Bibevski & Dunlap, 2011; Hardwick *et al.* 2012), are associated with chronic ischaemic heart disease or congestive heart failure and probably contribute to the evolution of these pathologies (Chen *et al.* 2001; Arora *et al.* 2003; Lopshire *et al.* 2009; Bibevski & Dunlap, 2011; Zucker *et al.* 2012; Nguyen *et al.* 2012; Shinohara *et al.* 2012).

Atrial arrhythmia induction

Heterogeneous activation of the cardiac nervous system can exert destabilizing influences on cardiac electrical indices (Armour *et al.* 2005; Scherlag *et al.* 2006; Billman, 2006). In response to mediastinal nerve stimulation, most IC neurons became excessively activated, including many previously inactive ones; such alteration in network behaviour preceded and persisted throughout such induced AF (Gibbons *et al.* 2012). We have previously shown that suppression of IC function via targeted neuromodulation therapy mitigates this MNS-induced AF potential (Gibbons *et al.* 2012).

In the current study we found that most IC neurons that responded to excessive MNS inputs likewise demonstrated preferential and extensive inputs from cardiopulmonary afferents. While some MNS-sensitive IC neurons received inputs from both the vagi and stellate ganglia, their response characteristics to central efferent autonomic inputs was not predictive of their potential contribution to local neuronal imbalance leading to AF induction. Based upon their integrated response to imposed afferent and efferent stressors, the data derived herein suggest that IC neurons that responded to MNS with enhanced activity were most likely made up of the convergent LCN population. Future studies should focus on which subpopulations of IC neurons are targeted by neuromodulation-based therapies, either electrical or pharmacological (Armour *et al.* 2005; Lopshire *et al.* 2009; Gibbons *et al.* 2012), for effective control of cardiac arrhythmias.

Myocardial ischaemia

Transient myocardial ischaemia impacts cardiomyocytes as well as neurons in multiple levels of the cardiac nervous system that regulate them (Waldmann *et al.* 2006; Southerland *et al.* 2007, 2012; Ardell *et al.* 2009).

The resultant local metabolic factors, coupled with reflex evoked changes in neurotransmitter release, are principal factors in augmenting the arrhythmogenic substrate, including the potential for sudden cardiac death, and subsequent apoptosis of affected myocytes within the ischaemic zone (Crow *et al.* 2004; Billman, 2006; Cohen & Downey, 2011; Southerland *et al.* 2012). As determined previously and confirmed here, myocardial ischaemia impacts IC neural network interactions, doing so primarily via cardiac afferent neuronal activation (Huang *et al.* 1993; Armour *et al.* 2002; Waldmann *et al.* 2006). Activation of ischaemic-sensitive afferent neurons can impact various elements within the ICNS (Foreman *et al.* 2000; Armour *et al.* 2002), even when they are disconnected from higher centres of the cardiac neuronal hierarchy (Huang *et al.* 1993). Data derived in this study demonstrate that myocardial ischaemia-transducing IC neurons which are preferentially influenced by cardiac afferent activation exhibit no selectivity with respect to central efferent neuronal inputs when compared to populations of non-ischaemic sensitive IC neurons. These data apparently reflect the differential processing capabilities of the ICNS convergent local circuit neuronal population. Recent studies have demonstrated that neuromodulation therapy has the potential to modulate arrhythmogenic and apoptotic potentials to ischaemic stressors (Southerland *et al.* 2007; Ardell *et al.* 2009; Lopshire *et al.* 2009; Southerland *et al.* 2012). Future studies should consider whether selective subpopulations of peripheral autonomic (intrathoracic extracardiac and intrinsic cardiac) neurons can be targeted therapeutically to provide cardioprotection in the presence of stressors.

Conclusion and significance

The data derived from these studies indicate that the intrinsic cardiac nervous system is composed of heterogeneous populations of neurons, as identified functionally in this report and in the past by anatomical means (Yuan *et al.* 1994; Armour *et al.* 1997; Parsons, 2004; Hoover *et al.* 2009), that act synergistically with one another and with neurons in intrathoracic extracardiac ganglia, the spinal cord, the brainstem and higher centres in the control of regional cardiac function (Brown, 1979; Zucker & Gilmore, 1991; Armour, 2008; McAllen *et al.* 2011; Southerland *et al.* 2012). Such an arrangement subtends in both normal and stressed states. The relative contribution of central *versus* peripheral aspects of the cardiac nervous system varies (Southerland *et al.* 2007, 2012; Lopshire *et al.* 2009; Zhang *et al.* 2009) according to the stressor applied (e.g. regional cardiac mechanical *vs.* ischaemic perturbations) and the adaptations so engendered in the neurohumoral control systems (Armour *et al.* 1998; Mill *et al.* 2011; Zucker *et al.*

2012; Hardwick *et al.* 2012). As such, neurons located in each level of the cardiac neuronal hierarchy (intrinsic cardiac, intrathoracic extracardiac and central) interact in an ongoing dynamic fashion to ensure adequate cardiac output that meets the demands imposed by transient alterations in bodily functions (Armour, 2008; Zucker *et al.* 2012).

This study makes evident the fact that the major population of intrinsic cardiac neurons involved in cardiac regulation is local circuit in nature. Thus for efferent control, while a limited population of identified IC neurons received direct centrally derived preganglionic inputs, a sizable population of intrinsic cardiac neurons transduced indirect inputs from one or more central neuronal sources (medulla *vs.* spinal cord neurons). As such, the population of LCNs that receive preferential but not direct central neuronal inputs, we have defined as secondary efferent LCNs. This subpopulation of IC neurons may subserve a major role in coordinating autonomic interactions on the target organ itself. Importantly, this population is probably involved in arrhythmia formation when its stochastic interactions become activated excessively.

A number of LCNs received preferential and divergent cardiopulmonary afferent inputs (Fig. 11). While some of the IC neurons that responded to touch or great vessel occlusions could be primary afferents, the majority exhibited wide-field distributions and responded to multi-modal inputs; these we define as secondary afferent LCNs. As such, this may be the population that becomes excessively activated in the transduction of ventricular ischaemia. In addition, it appears that the network interactions that occur among the various LCN populations distributed throughout the ICN do so primarily via the convergent LCN population.

Under basal conditions the low level, stochastic interactivity that occurs among the different ICN populations apparently acts to coordinate regional cardiac function. Yet, asymmetric changes in afferent or efferent inputs to that population can evoke disorganized responses with resultant imbalances in efferent distributions to tissues throughout the heart (Armour *et al.* 2005; Issa *et al.* 2005; Scherlag *et al.* 2005). Such a state can readily lead to cardiac arrhythmia induction (Scherlag *et al.* 2006; Billman, 2006; Armour, 2008). By inference, stabilization of IC/LCN stochastic interactivity may represent a novel approach for the suppression of atrial arrhythmia formation (Gibbons *et al.* 2012). Centrally mediated coordination of disparate IC neuronal networks likewise may find applications in the therapeutic management of compromised contractile function, such as occurs during the evolution of chronic heart failure with its attendant abnormal neurohumoral engagement (Lopshire *et al.* 2009; Zucker *et al.* 2012; Liu *et al.* 2012). Future studies should consider the contribution of differential remodelling of select neuronal

populations within the cardiac neuronal hierarchy in response to evolution of cardiac pathology in order to exploit potential neural targets to mitigate the adverse consequences of abnormal cardiac neuronal hierarchy function that attends cardiac disease.

Appendix. Significance of changes in firing rate

Changes identified in neuronal activity were compared at different time windows by calculating the average firing rate over time. The significance level of the observed differences in firing rate was assessed using a statistical test recently utilized in a study of primary motor cortex neurons (Shin *et al.* 2010). The resulting *P* value is a function of four parameters: the duration of the two time windows and the number of firings in each time window.

The null hypothesis is that the two firing rates are equal. For this analysis, it is assumed that the number of action potentials identified follows a Poisson distribution in each time window and that the difference in the activities follows a Skellam distribution (Skellam, 1946; Strackee & Deneir van der Gon, 1962). Parameters can then be estimated using the maximum likelihood approach. From the Skellam cumulative distribution function, the probability that the difference in number of firings is larger than the observed value provides the desired *P* value (unilateral test). The test was implemented in Matlab and adapted from the R package 'skellam' by Jerry W. Lewis. Two significance levels were used: 1% and 5%. Figure 2 shows the firing rate-dependent thresholds of significant increase and decrease of firing rate. Note that when the duration of the time windows are different the regions are asymmetric (Fig. 2B).

The advantages of this method are its simplicity, the robustness of its parameter estimation and its applicability in the case of low firing rates, including when the firing rate is zero. Its limitations are the assumptions of stationarity and Poisson-distributed firings. In contrast with cortical neurons, neurons in the right atrium ganglionated plexus tend to fire at low frequency unless a special event (e.g. atrial fibrillation) occurs. As a result, the limited number of firings in the time windows prevents robust estimation of a larger number of parameters.

References

- Adams DJ & Cuevas J (2004). Electrophysiological properties of intrinsic cardiac neurons. In *Basic and Clinical Neurocardiology*, ed. Armour JA & Ardell JL, pp. 1–60. Oxford University Press, New York.
- Andresen MC, Kunze DL & Mendelowitz D (2004). Central nervous system regulation of the heart. In *Basic and Clinical Neurocardiology*, ed. Armour JA & Ardell JL, pp. 187–219. Oxford University Press, New York.
- Ardell JL (2004). Intrathoracic neuronal regulation of cardiac function. In *Basic and Clinical Neurocardiology*, ed. Armour JA & Ardell JL, pp. 118–152. Oxford University Press, New York.
- Ardell JL, Butler CK, Smith FM, Hopkins DA & Armour JA (1991). Activity of in vivo atrial and ventricular neurons in chronic decentralized canine hearts. *Am J Physiol Heart Circ Physiol* **260**, H713–H721.
- Ardell JL, Cardinal R, Vermeulen M & Armour JA (2009). Dorsal spinal cord stimulation obtunds the capacity of intrathoracic extracardiac neurons to transduce myocardial ischemia. *Am J Physiol Regul Integr Comp Physiol* **297**, R470–R477.
- Ardell JL & Randall WC (1986). Selective vagal innervation of sinoatrial and atrioventricular nodes in canine heart. *Am J Physiol Heart Circ Physiol* **251**, H764–H773.
- Armour JA (2008). Potential clinical relevance of the 'little brain' on the mammalian heart. *Exp Physiol* **93**, 165–176.
- Armour JA, Collier K, Kember G & Ardell JL (1998). Differential selectivity of cardiac neurons in separate intrathoracic autonomic ganglia. *Am J Physiol Regul Integr Comp Physiol* **274**, R939–R949.
- Armour JA & Hopkins DA (1990). Activity of in vivo ventricular neurons. *Am J Physiol Heart Circ Physiol* **258**, H326–H336.
- Armour JA & Janes RD (1988). Neuronal activity recorded extracellularly from *in situ* mediastinal ganglia. *Can J Physiol Pharmacol* **66**, 119–127.
- Armour JA & Kember G (2004). Cardiac sensory neurons. In *Basic and Clinical Neurocardiology*, ed. Armour JA & Ardell JL, pp. 79–117. Oxford University Press, New York.
- Armour JA, Linderroth B, Arora RC, DeJongste MJL, Ardell JL, Kingma JG, Hill M & Foreman RD (2002). Long-term modulation of the intrinsic cardiac nervous system by spinal cord neurons in normal and ischaemic hearts. *Auton Neurosci* **95**, 71–79.
- Armour JA, Murphy DA, Yuan BX, MacDonald S & Hopkins DA (1997). Gross and microscopic anatomy of the human intrinsic cardiac nervous system. *Anat Rec* **247**, 289–298.
- Armour JA, Richer LP, Pagé PL, Vinet A, Kus T, Vermeulen M, Nadeau R & Cardinal R (2005). Origin and pharmacological response of atrial tachyarrhythmias induced by activation of mediastinal nerves in canines. *Auton Neurosci* **118**, 68–78.
- Arora RC, Cardinal R, Smith FM, Ardell JL, Dell'Italia LJ & Armour JA (2003). Intrinsic cardiac nervous system in tachycardia induced heart failure. *Am J Physiol Regul Integr Comp Physiol* **285**, R1212–R1223.
- Bibevski S & Dunlap ME (2011). Evidence for impaired vagus nerve activity in heart failure. *Heart Fail Rev* **16**, 129–135.
- Billman GE (2006). A comprehensive review and analysis of 25 years of data from an in vivo canine model of sudden cardiac death: Implications for future anti-arrhythmic drug development. *Pharmacol Ther* **111**, 808–835.
- Brown AM (1979). Cardiac reflexes. In *Handbook of Physiology*, section 2, *The Cardiovascular System*, vol. 1, *The Heart*, ed. Berne RM, Sperelakis N & Geiger SR, pp. 677–689. American Physiological Society (Williams and Wilkins), Bethesda.

- Cardinal R, Pagé P, Ardell JL & Armour JA (2009). Spatially divergent cardiac responses to nicotinic stimulation of ganglionated plexus neurons in the canine heart. *Auton Neurosci* **145**, 55–62.
- Chen P-S, Chen LS, Cao J-M, Sharifi B, Karagueuzian HS & Fishbein MC (2001). Sympathetic nerve sprouting, electrical remodeling and the mechanisms of sudden cardiac death. *Cardiovasc Res* **50**, 409–416.
- Cohen MV & Downey JM (2011). Ischemic postconditioning: from receptor to end-effector. *Antioxid Redox Signal* **14**, 821–831.
- Crow MT, Mani K, Nam YJ & Kitsis RN (2004). The mitochondrial death pathway and cardiac myocyte apoptosis. *Circ Res* **95**, 957–970.
- Dell'Italia LJ & Ardell JL (2004). Sympathetic nervous system in the evolution of heart failure. In *Basic and Clinical Neurocardiology*, ed. Armour JA & Ardell JL, pp. 340–367. Oxford University Press, New York.
- Foreman RD, Linderth B, DeJongste MJL, Ardell JL & Armour JA (2000). Central and peripheral mechanisms evoked by spinal cord stimulation (SCS) for angina pectoris. In *Management of Acute and Chronic Pain*, ed. Krames E & Reig E, pp. 597–604.
- Furukawa Y, Hoyano Y & Chiba S (1996). Parasympathetic inhibition of sympathetic effects on sinus rate in anesthetized dogs. *Am J Physiol Heart Circ Physiol* **271**, H44–H50.
- Gagliardi M, Randall WC, Bieger D, Wurster RD, Hopkins DA & Armour JA (1988). Activity of in vivo canine cardiac plexus neurons. *Am J Physiol Heart Circ Physiol* **255**, H789–H800.
- Gibbons DD, Southerland EM, Hoover DB, Beaumont E, Armour JA & Ardell JL (2012). Neuromodulation targets intrinsic cardiac neurons to attenuate neuronally mediated atrial arrhythmias. *Am J Physiol Regul Integr Comp Physiol* **302**, R357–R364.
- Gray AL, Johnson TA, Ardell JL & Massari VJ (2004a). Parasympathetic control of the heart. II. A novel interganglionic intrinsic cardiac circuit mediates neural control of the heart. *J Appl Physiol* **96**, 2273–2278.
- Gray AL, Johnson TA, Lauenstein JM, Newton SS, Ardell JL & Massari VJ (2004b). Parasympathetic control of the heart. III. Neuropeptide Y-immunoreactive nerve terminals synapse on three populations of negative chronotropic vagal preganglionic neurons. *J Appl Physiol* **96**, 2279–2287.
- Hardwick JC, Southerland EM, Girasole AE, Ryan SE, Negrotto S & Ardell JL (2012). Remodeling of intrinsic cardiac neurons: effects of β -adrenergic receptor blockade in guinea pig models of chronic heart disease. *Am J Physiol Regul Integr Comp Physiol* **303**, R950–R958.
- Herring N & Paterson DJ (2009). Neuromodulators of peripheral cardiac sympatho-vagal balance. *Exp Physiol* **94**, 46–53.
- Hoover DB, Isaacs ER, Jacques F, Hoard JL, Pagé P & Armour JA (2009). Localization of multiple neurotransmitters in surgically derived specimens of human atrial ganglia. *Neuroscience* **164**, 1170–1179.
- Huang MH, Ardell JL, Hanna BD, Wolf SG & Armour JA (1993). Effects of transient coronary artery occlusion on canine intrinsic cardiac neuronal activity. *Integr Physiol Behav Sci* **28**, 5–21.
- Issa ZF, Zhou X, Ujhelyi MR, Rosenberger J, Bhakta D, Groh WJ, Miller JM & Zipes DP (2005). Thoracic spinal cord stimulation reduces the risk of ischemic ventricular arrhythmias in a post-infarction heart failure canine model. *Circulation* **111**, 3217–3220.
- Kember G, Fenton GA, Armour JA & Kalyaniwalla N (2001). Competition model for aperiodic stochastic resonance in a Fitzhugh-Nagumo model of cardiac sensory neurons. *Phys Rev E Stat Nonlin Soft Matter Phys* **63**, 1–6.
- Langley G (1921). *The Autonomic Nervous System* Cambridge University Press, Cambridge, UK.
- Liu Y, Yue WS, Liao SY, Zhang Y, Au KW, Shuto C, Hata C, Park E, Chen P, Siu CW & Tse HF (2012). Thoracic spinal cord stimulation improves cardiac contractile function and myocardial oxygen consumption in a porcine model of ischemic heart failure. *J Cardiovasc Electrophysiol* **23**, 534–540.
- Lopshire JC, Zhou X, Dusa C, Ueyama T, Rosenberger J, Courtney N, Ujhelyi M, Mullen T, Das M & Zipes DP (2009). Spinal cord stimulation improves ventricular function and reduces ventricular arrhythmias in a canine postinfarction heart failure model. *Circulation* **120**, 286–294.
- McAllen RM, Salo LM, Paton JFR & Pickering AE (2011). Processing of central and reflex vagal drives by rat cardiac ganglion neurones: an intracellular analysis. *J Physiol* **589**, 5801–5818.
- McGuirt AS, Schmachet DC & Ardell JL (1997). Autonomic interactions for control of atrial rate are maintained after SA nodal parasympathectomy. *Am J Physiol Heart Circ Physiol* **272**, H2525–H2533.
- Mill JG, Stefanon I, dos Santos L & Baldo MP (2011). Remodeling in the ischemic heart: the stepwise progression for heart failure. *Braz J Med Biol Res* **44**, 890–898.
- Nguyen BL, Li H, Fishbein MC, Lin SF, Gaudio C, Chen PS & Chen LS (2012). Acute myocardial infarction induces bilateral stellate ganglia neural remodeling in rabbits. *Cardiovasc Pathol* **21**, 143–148.
- Parsons RL (2004). Mammalian cardiac ganglia as local integration centers: histochemical and electrophysiological evidence. In *Neural Mechanisms of Cardiovascular Regulation*, ed. Dun NJ, Machado BH & Pilowsky PM, pp. 335–356. Kluwer Academic Publishers, Boston.
- Randall DC, Brown DR, Li SG, Olmstead ME, Kilgore JM, Sprinkle AG, Randall WC & Ardell JL (1998). Ablation of posterior atrial ganglionated plexus potentiates sympathetic tachycardia to behavioral stress. *Am J Physiol Regul Integr Comp Physiol* **275**, R779–R787.
- Randall DC, Brown DR, McGuirt AS, Thompson G, Armour JA & Ardell JL (2003). Interactions within the intrinsic cardiac nervous system contribute to chronotropic regulation. *Am J Physiol Regulatory Integrative Comp Physiol* **285**, R1066–R1075.
- Richer LP, Vinet A, Kus T, Cardinal R, Ardell JL & Armour JA (2008). α -Adrenoceptor blockade modifies neurally induced atrial arrhythmias. *Am J Physiol Regul Integr Comp Physiol* **295**, R1175–R1180.
- Scherlag BJ, Nakagawa JH, Jackman WM, Yamanashi WS, Patterson E, Po S & Lazzara R (2005). Electrical stimulation to identify neural elements on the heart: their role in atrial fibrillation. *J Interv Card Electrophysiol* **13** (Suppl. 1), 37–42.

- Scherlag BJ, Patterson E & Po SS (2006). The neural basis of atrial fibrillation. *J Electrophysiol* **39**, S180–S183.
- Schwartz PJ, La Rovere MT & Vanoli E (1992). Autonomic nervous system and sudden cardiac death. Experimental basis and clinical observations for post-myocardial infarction risk stratification. *Circulation* **85**, I77–I91.
- Shen MJ, Choi E-K, Tan AY, Han S, Shinohara T, Maruyama M, Chen LS, Shen C, Hwang C, Lin S-F & Chen P-S (2011). Patterns of baseline autonomic nerve activity and development of pacing-induced atrial fibrillation. *Heart Rhythm* **8**, 583–589.
- Shin HC, Aggarwal V, Acharya S, Schieber MH & Thakor NV (2010). Neural decoding of finger movements using Skellam-based maximum-likelihood decoding. *IEEE Trans Biomed Eng* **57**, 754–760.
- Shinohara T, Shen MJ, Han S, Maruyama M, Park HW, Fishbein MC, Shen C, Chen PS & Lin SF (2012). Heart failure decreases nerve activity in the right atrial ganglionated plexus. *J Cardiovasc Electrophysiol* **23**, 404–412.
- Skellam JG (1946). The frequency distribution of the difference between two Poisson variates belonging to different populations. *J R Stat Soc Ser A* **109**, 296.
- Southerland EM, Gibbons DD, Smith SB, Sipe A, Williams CA, Beaumont E, Armour JA, Foreman RD & Ardell JL (2012). Activated cranial cervical cord neurons affect left ventricular infarct size and the potential for sudden cardiac death. *Auton Neurosci* **169**, 34–42.
- Southerland EM, Milhorn D, Foreman RD, Linderorth B, DeJongste MJL, Armour JA, Subramanian V, Singh M, Singh K & Ardell JL (2007). Preemptive, but not reactive, spinal cord stimulation mitigates transient ischemia-induced infarction via cardiac adrenergic neurons. *Am J Physiol Heart Circ Physiol* **292**, H311–H317.
- Strackee J & Deneir van der Gon JJ (1962). The frequency distribution of the difference between two Poisson variates. *Stat Neerl* **16**, 17–23.
- Taylor EW, Jordan D & Coote JH (1999). Central control of the cardiovascular and respiratory systems and their interactions in vertebrates. *Physiol Rev* **79**, 855–915.
- Thompson GW, Collier K, Ardell JL, Kember G & Armour JA (2000). Functional interdependence of neurons in a single canine intrinsic cardiac ganglionated plexus. *J Physiol* **528**, 561–571.
- Vanoli E, Adamson PB, Foreman RD & Schwartz PJ (2008). Prediction of unexpected sudden death among healthy dogs by a novel marker of autonomic neural activity. *Heart Rhythm* **5**, 300–305.
- Waldmann M, Thompson GW, Kember G, Ardell JL & Armour JA (2006). Stochastic behaviour of atrial and ventricular intrinsic cardiac neurons. *J Applied Physiol* **101**, 1–7.
- World Medical Association; American Physiological Society (2002). Guiding principles for research involving animals and human beings. *Am J Physiol Regul Integr Comp Physiol* **283**, R281–R283.
- Yuan BX, Ardell JL, Hopkins DA & Armour JA (1993). Differential cardiac responses induced by nicotine sensitive canine atrial and ventricular neurons. *Cardiovasc Res* **27**, 760–769.
- Yuan BX, Ardell JL, Hopkins DA, Losier AM & Armour JA (1994). Gross and microscopic anatomy of the canine intrinsic cardiac nervous system. *Anat Rec* **239**, 75–87.
- Zhang Y, Popovic ZB, Bibevski S, Fakhry I, Sica DA, Van Wagoner DR & Mazgalev TN (2009). Chronic vagus nerve stimulation improves autonomic control and attenuates systemic inflammation and heart failure progression in a canine high-rate pacing model. *Circ Heart Fail* **2**, 692–699.
- Zucker IH & Gilmore JP (1991). *Reflex Control of the Circulation*. CRC Press, Boca Raton.
- Zucker IH, Patel KP & Schultz HD (2012). Neurohumoral stimulation. *Heart Fail Clin* **8**, 87–99.

Additional information

Competing interests

None declared.

Author contributions

J.L.A., J.A.A., E.B. and E.M.S. designed and performed the experiments. Experiments were done at Quillen College of Medicine, East Tennessee State University, Johnson City, TN. V.J. and A.V. developed the signal processing methodology. S.S. implemented the signal processing tools. J.L.A., S.S. and E.B. analysed the data. All authors contributed to writing the paper and approved the final version of the manuscript.

Funding

This work was supported by NIH grant HL71830 (to J.L.A.), by the Natural Sciences and Engineering Research Council of Canada (V.J.), by the Fonds de Recherche du Québec – Santé (V.J.) and by a graduate fellowship from the Centre for Applied Mathematics in Bioscience and Medicine at McGill University (S.S.).

Acknowledgements

None.